Asian Journal of Green Chemistry 10 (2026) 565-588

Asian Journal of Green Chemistry

Original Research Article View Article Online | View Journal

Evaluation of Anti-Asthmatic Potential of *Emblica Officinalis* Seed Extract in RAW 264.7 Cell Lines

Elango Kannan [1,*], Mumtha Logesh[1,2], Priyadharshini S[2]

[1]*Faculty of Pharmacy, Karpagam Academy of Higher Education, Coimbatore- 641 105, Tamil Nadu, India*
[2]*Department of Pharmacognosy, JSS College of Pharmacy, JSS Academy of Higher Education and Research, Ooty, Nilgiris-643001, Tamil Nadu, India*

ARTICLE INFORMATION

Submitted: 2025-10-18
Revised: 2025-11-21
Accepted: 2026-01-22
Published: 2026-01-26
Manuscript ID: AJGC-2510-1848
DOI: 10.48309/ajgc.2026.553890.1848

KEYWORDS

Antiasthmatic activity
Emblica officinalis
Seed extract
RAW 264.7 cell line
LPS induced

ABSTRACT

This study aims to explore the anti-asthmatic potential of *Emblica officinalis* seed extract by assessing its effect on inflammatory markers in RAW 264.7 cell line. The preliminary evaluation of *Emblica officinalis* seed extract performed and characterized by UV, HPLC, and GCMS. Molecular docking was carried out using Schrodinger. DPPH, ABTS, and nitric oxide production were determined to study antioxidant effects, and cytotoxicity was assessed by MTT assay. The expression of IL-4, IL-13, TNF-alpha in LPS induced RAW 264.7 cell lines was analyzed using FACS method. The hydroalcoholic extract produced an extractive and ash values of 2.85% w/w and 3.47 ± 0.15% w/w, respectively. The determination of total phenolic and flavonoid content was favorable. The characterization of the extract was performed and analyzed through HPLC chromatograms. The GCMS chromatogram showed peaks at various retention times, indicating the presence of phytoconstituents. *In silico* studies showed good interactions between selected ligands and the target proteins. The antioxidant studies proved that the extract possesses free radical scavenging activity, reduces nitric oxide production, and MDA levels. The extract proved to be non-toxic in the MTT assay. In LPS induced RAW 264.7 cells the expression of the target proteins that actively involved in the pathogenesis of asthma was decreased.

Corresponding author, E-mail: elango.kannan@kahedu.edu.in (E. Kannan).
Tel.: +9443257859.

Graphical Abstract

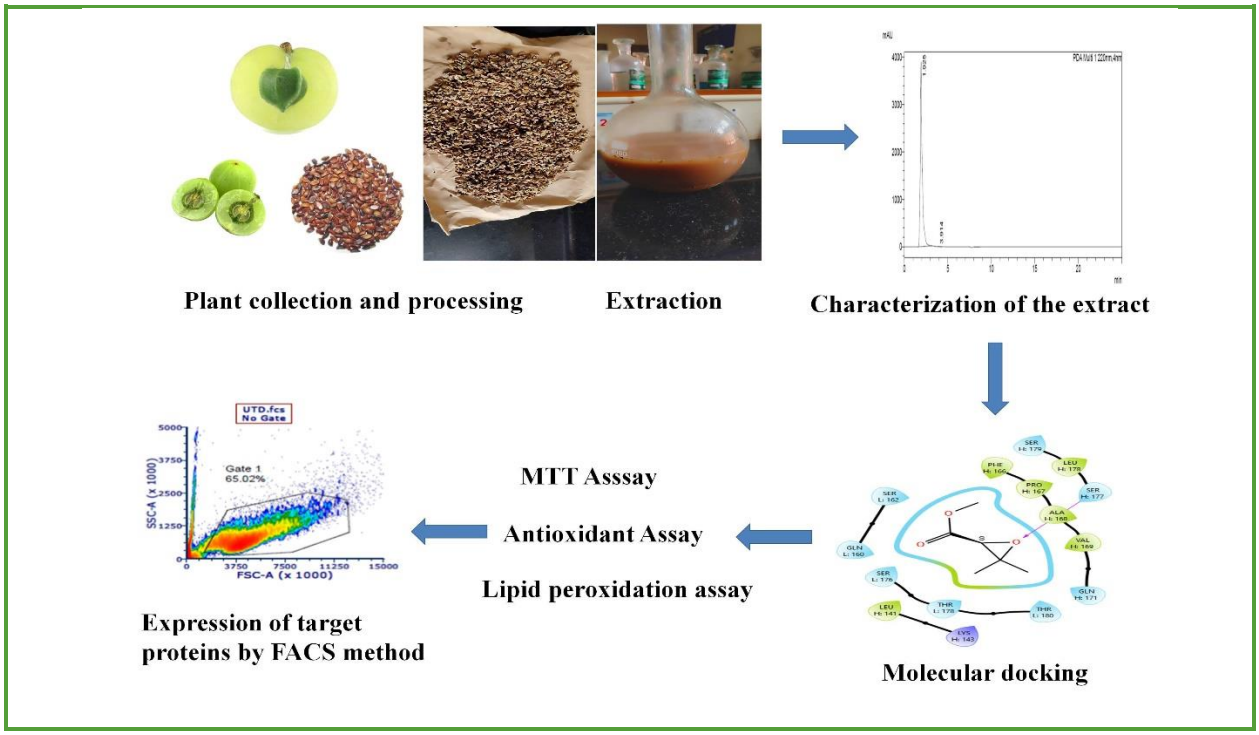

Introduction

Allergic asthma, a chronic inflammatory disease of the airways that is becoming increasingly prevalent and responsible for 0.4 million deaths each year, affects over 350 million people globally [1–7]. Along with its financial implications [1,8–11], the disease can lead to a marked deterioration in quality of life, especially in cases of severity and lack of control. To begin with, asthma can be categorized into two primary subtypes: Th2-low, or non-type 2 asthma, and Th2-high, or type 2 asthma [7]. Type 2 asthma is characterized by the presence of Th2 cytokines, especially interleukin (IL)-4, IL-5, and IL-13 [1,3,12]. This condition involves dendritic cells, type 2 innate lymphoid cells (ILC2), smooth muscle cells, M2 macrophages, epithelial cells, fibrocytes, smooth muscle cells, Th2 lymphocytes, and natural killer (NK)-T cells that produce type 2 cytokines, eosinophils and mast cells. Asthma is marked by bronchial hyperresponsiveness (BHR), airway inflammation, mucus obstruction, and airway remodeling, leading to symptoms such as respiratory distress, wheezing chest tightness, coughing, intolerance to exercise and sputum production [6,13,14]. Remarkably, a significant number of difficult to treat asthma patients present with chronic type 2 inflammation, in spite of the high sensitivity of Th2 cells for suppression by corticosteroids—the promising drugs for asthma. According to emerging research, patients with uncontrolled asthma have higher levels of ILC2s and Th2 cells, which can develop corticosteroid-resistant states [1]. In an effort to create new molecules, the so-called "asthma endotypes" have been defined in light of the disease's complexity and heterogeneity [8,15,16].

Interleukins (IL)-4 and -13 play key roles in type-2 asthma. IL-4 is significantly involved in Th2 cell differentiation, immunoglobulin class switching and eosinophil trafficking. IL-13

works with IL-4 in promoting IgE synthesis and also induces nitric oxide production, fibroblast proliferation, and goblet cell metaplasia. Furthermore, elicits hyperplasia of airway smooth muscle cells and contractile responses. In type-2 asthma, cytokines cause bronchial inflammation and remodeling. IL-13 is responsible for airway hyper-responsiveness, mucus hyperproduction, and changes in bronchial structure. Thus, both IL-13 and IL-4 actively participate in the initiation of bronchial epithelial dysfunction, which is a hallmark symptom of asthma [17-19]. Levels of IL-4, IL-5, and IL-13 in sputum and BALF are higher in the asthmatic population. One pleiotropic Th1 cytokine that plays a major role in the pathophysiology of asthma is tumor necrosis factor-α (TNF-α). Severe asthma and neutrophilic asthma have elevated TNF-α expression. TNF-α encourages the recruitment of neutrophils by activating cytokines. Nevertheless, TNF-α might also play a role in the synthesis of Th2 cytokines like IL-4, IL-5, and IL-13. Moreover, TNF-α increases the contraction of smooth muscles in the airways, causing hyper-responsiveness [20]. The present research is focused on finding a complementary alternative medicine; in this, the seeds of *Emblica officinalis* Gaertn belonging to the family Euphorbiaceae have been selected based on ethnobotanical claims by tribal community for respiratory disorders. The phytoconstituents present in the seeds may have the activity against asthma [21,22]. Hence, the study aims to investigate the constituents present in hydroalcoholic extracts of seeds and to estimate their antiasthmatic activity [23,24].

Materials and Methods

Materials

Cell line: Raw 264.7 (murine macrophage cell line, NCCS, Pune), Cell culture medium: DMEM high glucose (#AL007A, Himedia), Fetal Bovine Serum (#RM10432, Himedia), Antibiotic Antimycotic Solution-Penicillin & Streptomycin (#A001A, Himedia), Trypsin-EDTA solution (#TCL155, Himedia), D-PBS (#TL1006, Himedia), DMSO (#PHR1309, Sigma), MTT Reagent (# 4060, Himedia), Paclitaxel (#RM9750, Himedia), T25 flask (#12556009, Biolite - Thermo), 96-well plate for culturing the cells (Corning, USA), 1.5 mL centrifuge tubes (TARSON), multichannel pipettes and a pipettor (#Eppendorf), 10 to 1,000 µL tips (TARSON), 50 mL centrifuge tubes (# 546043 TARSON), adjustable pipettes (2-10 µL, 10-100 µL, and 100-1,000 µL).

Methods

Collection and authentication of plant material

Fruits of the *Emblica officinalis* plant were gathered in January 2010 from the Nilgiri district in Tamil Nadu, India. The obtained plant was verified by Dr. S.P. Subramani, a botanist and Chief Technical Officer of the Indian Council of Forestry Research and Education's Institute of Forest Genetics and Tree Breeding in Coimbatore. For future use, the voucher specimen has been stored in the lab (333/FRC/ID/FECC/IFGTB/2024).

Extractive value

2 g of the coarsely powdered dried seed of *Emblica officinalis* was weighed using a weighing balance and transferred into a dry stoppered conical flask (250 mL). Then the flask was filled with ethanol and water (30 mL) and stored at room temperature for 24 h with frequent shaking. Then filter the mixture using Whatman No. 1 filter paper. The resulting filtrate was shifted into a Petri plate that had been previously weighed. By completely evaporating the solvent, the resulting extract was dried out. Using the

following formula, the extractive value was computed as a percentage and noted [25]: (Weight of dried extract/Weight of plant material) × 100 = extractive value (%)).

Ash value

A silica crucible was filled up that had been previously mixed with 2 g of powdered dried *Emblica officinalis* material. In the crucible, the material was distributed in an even layer. The temperature was gradually increased to 500–600 °C until free of carbon. After cooling, the crucible was weighed. The percentage of ash in relation to the air-dried plant material was used to compute the total ash [26].

Extraction of plant material

The 300 g of P. emblica seeds were removed from the fruits, shade-dried, and milled with a milling machine. They were extracted through a cold maceration process with absolute ethanol (99.5%) and distilled water in a 30:70 ratio, involving intermittent shaking for 10 days and filtration. The solvent was evaporated at a maximum temperature of 55 °C using a rotary evaporator (Rota vapor, R-210/215, Buchi, Switzerland) under reduced pressure. The concentrated semi-solid material was dried in a desiccator to produce dark green hydroalcoholic, or HAE, which is now 3.28% on the dry weight. Qualitative phytochemical studies were performed on the extract [27].

Phytochemical analysis

The preliminary phytochemical tests were performed for the hydroalcoholic extract of *Emblica officinalis* seeds to identify the presence of alkaloids, steroids and sterols, glycosides, saponins, flavonoids, tannins, proteins, amino acids, fatty acids, and resins [27-30].

Determination of total phenolic and flavonoid content

The Folin-Ciocalteu technique was used to calculate the total phenolic content. At 765 nm, the absorbance was measured. A standard calibration curve was obtained using gallic acid (15–120 mg/mL). The results were reported as gallic acid equivalents/mg of extract dry weight. The aluminum chloride colorimetric technique was used to determine the total flavonoid levels. Absorbance at 510 nm was measured for the mixture three times. The results were shown as rutin per mg/g of extract's dry weight [31].

Characterization of the hydroalcoholic extract

Due to the fact that plant extracts usually occur as a combination of phytoconstituents, the extract was subjected to UV and HPLC to study the active compounds present [32]. Phytoconstituents present in the extract were recognized by GC-MS associating the results of the mass spectrum with the inbuilt NIST library database [33].

Molecular docking

A molecular docking study was performed using Schrodinger version 2024 – 1, for the compounds identified by the characterization of the extract using GC-MS with the targets IL-4, IL-13 and TNF-α. According to their binding affinities and interaction patterns the following compounds given below were determined to be the most promising candidates among the compounds evaluated [34].

Preparation of ligand

The ChemDraw program was used to generate the ligand structure (Table 1), and the Discovery Studio visualizer was used to create its three-dimensional structures.

Table 1. Preparation of ligand structure with ChemDraw

Vinyl crotonate	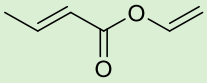	**Vinyl crotonate**	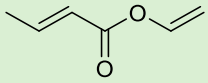
3-Hexen-2-one,3-methyl	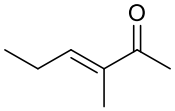	Acetic acid cyano	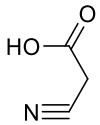
Borane, Methyl dipropyl	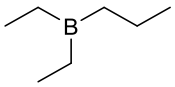	Borane trimethyl	
Borane, *tris* (1-methylethyl)	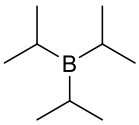	3-Methyl -1,2 diazinine	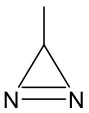
3-Methyl-3-nitrobut-1-ene	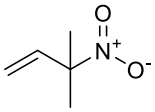	Propanal, 2,3-Dihydroxy-,(*S*)-	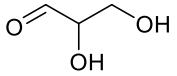
Prenyl bromide	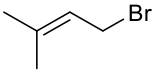	1-Butanamine	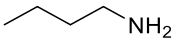
Acetonitrile		Oxalic acid, Allylethyl ester	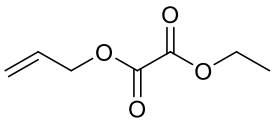
Methyl isocyanide		1-Propanamine, *N*,2-dimethyl-*N*-nitroso	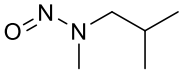
Borane carbonyl	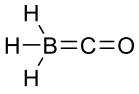	3,3-Dimethyloxirane-2-carboxylic acid, methyl ester	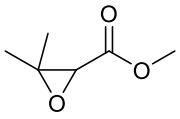

Receptor protein preparation

SwissPDB Viewer was used to study the protein structures, which were retrieved from the Protein Data Bank. For the purpose of study, target proteins such TNF-α (PBD ID: 2AZ5), IL-4 (PBD ID: 2B8U), and IL-13 (PBD ID: 4I77) were produced.

Molecular docking

Using the Discovery Studio visualizer, the 2D and 3D structures of ligands and receptor proteins were created, and predictions such as the docking score, binding affinity, and hydrogen bonding between the target proteins' amino acid pockets were studied.

In vitro studies

DPPH assay

100 µL of the test substance at various concentrations (10, 20, 40, 60, 80, and 100 µg/mL) was added to the wells. Each well

received 100 µL of 0.1 mM DPPH reagent (4 mg/100 mL), bringing the amount of the reaction mixture to 200 µL. The reaction was then dark-incubated for 30 min at room temperature. A spectrophotometer was used to measure the absorbance at 515 nm. The linear equation Y= M(x) + C was used to calculate the IC_{50} value. Here, Y= 50; M and C values were derived from the scavenging activity [35-37].

ABTS activity assay

7 mM ABTS was prepared in water and radical cation generation was done by adding 2.45 mM potassium persulfate to the stock solution and incubating at room temperature for 12 to 16 h in the dark. After that, PBS (pH 7.4) was used to dilute the ABTS until it had an absorbance of 0.7 at 750 nm.

Additionally, 100 µL of the test compound at various concentrations (10, 20, 40, 60, 80, and 100 µg/mL) was added to each well. Next, 100 µL of the reagent that made up the reaction mixture was added to 200 µL, and the plates were shaken for 10 seconds at a medium speed. At 750 nm, the absorbance was measured with a spectrophotometer. The logarithmic equation, Y= Mx+C, and linear regression were used to calculate the IC_{50} value. The scavenging activity graph was used to determine the M and C values for Y = 50 in this case [38,39].

MTT assay

The MTT assay is a colorimetric method for determining cell proliferation and cytotoxicity, by reducing the yellow, water-soluble tetrazolium dye MTT into formazan crystals, which turn purple when dissolved in the appropriate solvent and whose intensity is proportional to the number of viable cells. At 570 nm, it can be detected spectrophotometrically. For the test, a 200 µL seed cell suspension is placed into a 96-well plate at the necessary cell density. Overnight, the cells were allowed to proliferate. The test agent was then added in the proper doses of 200, 400, 600, 800, and 1,000 (µg/mL) and incubated for 24 h at 37 °C in an environment with 5% CO_2. After the incubation period, MTT reagent was added to the spent media at a concentration of 0.5 mg/mL of total volume, but only for adherent cell lines. After that, the plate was covered with aluminum foil and left to incubate for 3 h. Lastly, to improve solubility, 100 µL of DMSO was added and gently swirled with a gyratory shaker. Using a reference wavelength, the absorbance was measured on a spectrophotometer at 570 and 630 nm. The logarithmic equation, Y=Mln (x) + C, and the linear regression equation, Y = Mx+C, were used to calculate the IC_{50} value. Here, the viability graph was used to obtain the M and C values for Y = 50 [40-42].

Nitric oxide inhibition

Cultured cells were seeded in 96 well plates at a density of 20,000 cells/well and incubated for the 24 h. After incubation, the cells were treated with given test compound at different concentrations (20, 40, 60, 80, and 100 µg/mL), except untreated (Negative Control) for 1 h.

Then, the cells were treated with 1 µg/mL LPS and incubated for 24 h. After incubation period, the supernatant was collected from all the wells and gently washed with cold PBS by centrifugation at 1,000 × g for 5 min. The whole supernatant was collected in the assay and transferred into a clean tube; the culture medium was used as a blank. The tubes were kept on ice and the experiment was performed based on EZ Assay Nitric Oxide Estimation Kit instructions. The average absorbance of each standard and sample was noted.

The corrected absorbance was calculated by subtracting the absorbance value of the standard A (0 µM) from itself and all other values (both

standards and samples). The corrected absorbance values of each standard as a function of $NaNO_2$ concentration were plotted. From the standard curve and by using formula, the values of total nitric oxide for each sample were determined [43-46].

Lipid peroxidation assay

Cultured cells were seeded in a 6-well plate with the density of 0.5 × 10^6 cells/well and incubated for 24 h. Later, the spent media was removed and the cells were treated with the test compounds (20, 40, 60, 80, and 100 µg/mL) for 24 h and then with H_2O_2 (1 mM) for 24 h.

Untreated cells were used as a Negative Control. Following the incubation phase, the cells were collected by trypsinization. The collected cells were used to estimate MDA levels by ELISA method, as per the manufacturer's instructions [47,48].

Anti-inflammatory effect of test compound (HAE) by analyzing IL-4, IL13, and TNF-alpha expression on LPS induced RAW 264.7 cell lines

Culture cells were transferred to a 96-well plate at a density of 5 × 10^5 cells/2 mL, and were incubated for 24 h at 37 °C in a CO_2 incubator. Then, the spent medium was and treated with LPS (1 µg/mL) for 3 h. 2 mL of culture media were then filled with the necessary concentrations of the experimental compounds and control, and the mixture was incubated for 24 h. LPS (1 µg/mL) is an inflammatory inducer; untreated cells serve as the negative control, and dexamethasone (5 µg/mL) is the standard. The medium from each well was aspirated and cleaned with PBS. Afterward, 2 mL of culture medium was added, and the cells were collected directly into 12 × 75 mm polystyrene tubes. The tubes underwent centrifugation for 5 min at 300 × g and a temperature of 25 °C. The supernatant was discarded, and PBS was used for washing. Subsequently, the PBS was entirely removed and 1 mL of cold 70% ethanol was used to fix the cells. The cell pellet added dropwise while vortexing and incubated for 30 min in a -20 ˚C freezer. The supernatant was discarded and pellets were carefully collected. Due to their increased buoyancy after fixation, the ethanol-fixed cells were spun at a higher centrifugal speed than the unfixed cells. The cells were washed with PBS and 10 µL of desired sample was added. The prepared mixture was thoroughly mixed and incubated for 0.5 h in the dark at room temperature (20-25 °C). Finally treated with 500 µL of DPBS and mixed. FACS was analyzed using FCS Express software [49-53].

Results

Physicochemical and phytochemical evaluation of Emblica officinalis seed extract

The preliminary evaluation of *Emblica officinalis* seed extract involves determination of extractive value, ash value, and phytochemical constituents. The hydroalcoholic extract yielded an extractive value of 2.85% w/w. The total ash content was determined to be 3.47 ± 0.15% w/w (mean ± SD, n = 3), indicating the absence of excessive extraneous earthy matter and adulterants. Phytochemical screening of the hydroalcoholic extract showed the presence of multiple bioactive compounds. The extract tested positive for proteins, alkaloids, saponins, phenols, tannins, flavonoids, phytosterols, fixed oils, and fats.

Total phenolic content quantification and characterization of the hydroalcoholic extract of Emblica officinalis seeds

Total phenolic and flavonoid content

The hydroalcoholic extract of *Emblica officinalis* seeds was evaluated for its total phenolic and flavonoid content. The total phenolic content, determined using the Folin Ciocalteu method and expressed in terms of gallic acid equivalents (GAE), was found to be 7.025 ± 0.025 mg/mL (gallic acid equivalent). The total flavonoid content, quantified by the aluminum chloride colorimetric method and expressed as rutin equivalents, was found to be 5.012 ± 0.007 mg/mL (rutin equivalent). This confirms the presence of key antioxidant phytochemicals in the extract.

UV spectral analysis

UV spectrophotometric analysis revealed two major absorption peaks for the extract at 253.70 nm (0.65 A) and 360.20 nm (0.13 A) (Table 2), suggesting the presence of conjugated systems typically associated with phenolic and flavonoid structures. These absorbance maxima further support the presence of UV-active phytoconstituents (Figure 1).

HPLC analysis and GC-MS profiling

The HPLC chromatogram at 220 nm showed two prominent peaks at retention times of 1.925 min and 3.914 min, with the first peak accounting for 99.97% of the total peak area. This indicates the presence of a major compound contributing to the extract's chemical profile, along with a minor constituent. Gas Chromatography–Mass Spectrometry (GC-MS) was used to analyze chemical composition of the hydroalcoholic extract of *Emblica officinalis* seeds. The chromatogram showed peaks at retention times (Rt) of 5.1 min, 7.2 min, and 7.8

Table 2. UV peaks obtained for the extract

Peak number	X (nm)	Y (A)
1	360.20	0.13
2	253.70	0.65

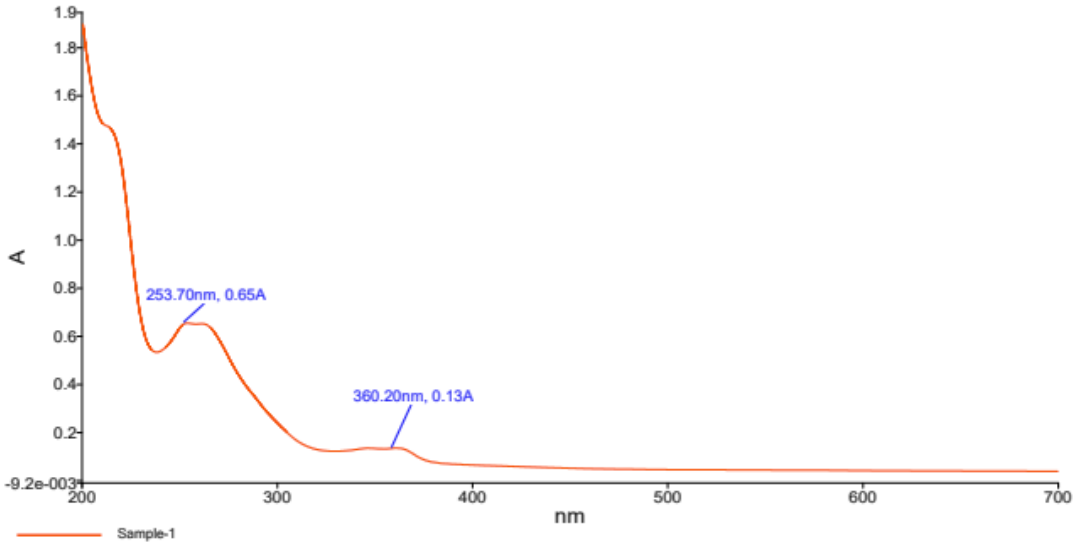

Figure 1. UV absorption spectra for the extract

min, indicating the presence of a diverse range of phytoconstituents. At Rt 5.1 min, compounds such as vinyl crotonate (6.90%), 3-hexen-2-one, 3-methyl (5.42%), borane, methyl dipropyl- (4.04%), and prenyl bromide (4.58%) were identified as shown in Table 3. At Rt 7.2 min, the major components included acetonitrile (48.9%), methyl iso-cyanide (26.7%), along with minor constituents like borane carbonyl, acetic acid cyano-, and 3-methyl-1,2-diazine shown in Table 4. The peak at Rt 7.8 min revealed compounds such as propanal, 2,3-dihydroxy-, (*S*)- (22.4%), 1-butanamine (12.2%), oxalic acid, allylethyl ester (5.07%), and 1-propanamine, *N*,2-dimethyl-*N*-nitroso (3.40%) given in Table 5. These identified phytoconstituents include esters, amines, nitriles, and borane derivatives (Figure 2).

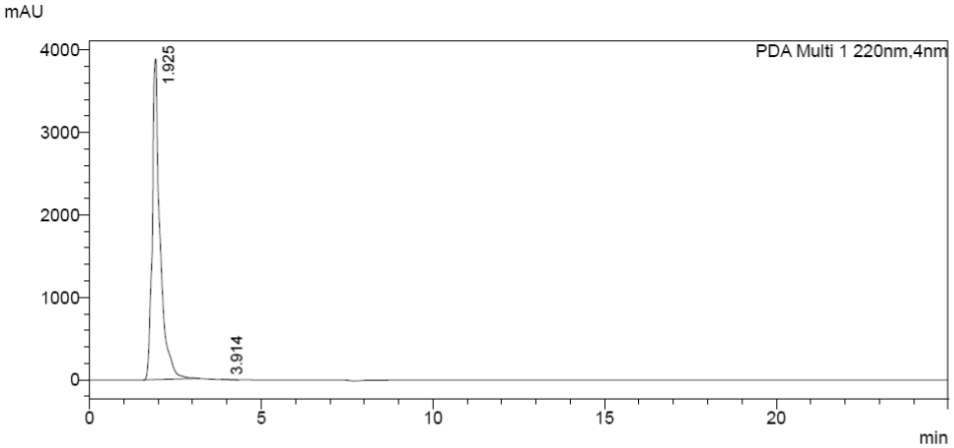

Figure 2. HPLC Chromatogram of *Emblica officinalis* seed extract showing 2 peaks at 220 nm

Table 3. Compounds identified in hydroalcoholic extract of *Emblica officinalis* seeds at Rt 5.1 from GC-MS chromatogram peaks

Compound	Rt	Peak area (%)	Molecular weight	Molecular formula	Structure
Vinyl crotonate	5.1	6.90	112	$C_6H_8O_2$	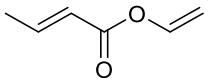
3-Hexen-2-one, 3-Methyl	5.1	5.42	112	$C_7H_{12}O$	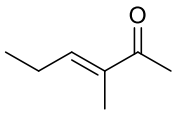
Borane, Methyl dipropyl-	5.1	4.04	112	$C_7H_{17}B$	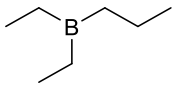
Borane, *tris* (1-methylethyl)-	5.1	3.18	140	$C_9H_{21}B$	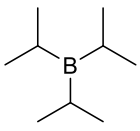
3-Methyl-3-nitrobut-1-ene	5.1	2.93	115	$C_5H_9NO_2$	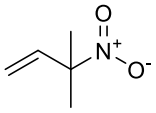
Prenyl bromide	5.1	4.58	148	C5H9Br	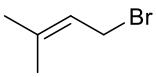

Table 4. Compounds identified in hydroalcoholic extract of *Emblica officinalis* seeds at Rt 7.2 from GC-MS chromatogram peaks

Compound	Rt	Peak area (%)	Molecular weight	Molecular formula	Structure
Acetonitrile	7.2	48.9	41	C_2H_3N	
Methyl isocyanide	7.2	26.7	41	C_2H_3N	
Borane carbonyl	7.2	4.96	42	CH_3BO	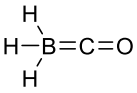
Acetic acid cyano-	7.2	4.19	85	$C_3H_3NO_2$	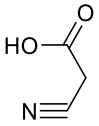
Borane trimethyl	7.2	5.37	56	C_3H_9B	
3-Methyl–1,2-diazinine	7.2	3.70	56	$C_2H_4N_2$	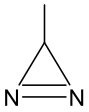

Table 5. Compounds identified in hydroalcoholic extract of *Emblica officinalis* seeds at Rt 7.8 from GC-MS chromatogram peaks

Compound	Rt	Peak area (%)	Molecular weight	Molecular formula	Structure
Propanal, 2,3-Dihydroxy-, (*S*)-	7.8	22.4	90	$C_3H_6O_3$	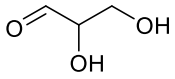
1-Butanamine	7.8	12.2	73	$C_4H_{11}N$	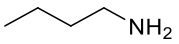
Oxalic acid, Allylethyl ester	7.8	5.07	158	$C_7H_{10}O_4$	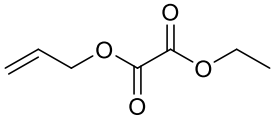
Borane carbonyl	7.8	3.68	42	CH_3BO	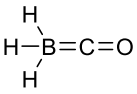
1-Propanamine, *N*,2-Dimethyl-*N*-nitroso	7.8	3.40	116	$C_5H_{12}N_2O$	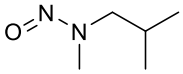
3,3-Dimethyloxirane-2-carboxylic acid, Methyl ester	7.8	3.13	130	$C_6H_{10}O_3$	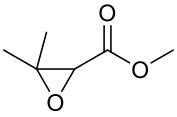

Molecular docking

Molecular docking studies were conducted using Schrodinger (version 2024-1) to evaluate the binding interactions of GC-MS-identified phytoconstituents from the hydroalcoholic extract of *Emblica officinalis* seeds with inflammatory cytokine targets such as TNF-α (PDB ID: 2AZ5), IL-4 (PDB ID: 2B8U), and IL-13 (PDB ID: 4I77) (Figure 3). Ligands were sketched in ChemSketch, and energy minimization was performed using Discovery Studio Visualizer. The receptor proteins were retrieved from the RCSB Protein Data Bank and preprocessed using SwissPDB Viewer. Among the docked compounds, Propanal, 2,3-dihydroxy-, (*S*)- exhibited the most promising interactions across all targets (Figure 4). For TNF-α, it exhibited a binding affinity of –3.780 kcal/mol and formed strong hydrogen bonds with residues TYR151, GLN61, and LEU120 (Figures 5 and 6), indicating a stable occupancy in the binding cavity (Tables 6-8). A comparatively weaker binder, 1-Butanamine, showed a binding score of –2.629 kcal/mol and lacked significant interactions, suggesting poor affinity. For comparison, Dexamethasone, the standard anti-inflammatory drug, exhibited a stronger binding affinity of –5.912 kcal/mol. Against IL-4, Propanal displayed a docking score of –3.524 kcal/mol (Table 6), forming stable hydrogen bonds with SER70, LYS76, and ASP125 (Figure 7). In the IL-13 receptor site, it bound with an energy of –3.446 kcal/mol (Table 7), establishing interactions with GLN85, TYR110, and ASP72 (Figure 5), thus stabilizing within the active site. The consistent interaction of Propanal across all targets suggests its potential as a multi-targeted anti-inflammatory candidate. Its favorable hydrogen bonding and spatial compatibility within the binding pockets of all three inflammatory mediators support its pharmacological relevance. Despite Dexamethasone showing superior affinity, Propanal, being a naturally occurring compound, may serve as a promising lead for further development. The overall findings highlight the ability of phytoconstituents in *Emblica officinalis* to modulate key inflammatory targets in biological systems.

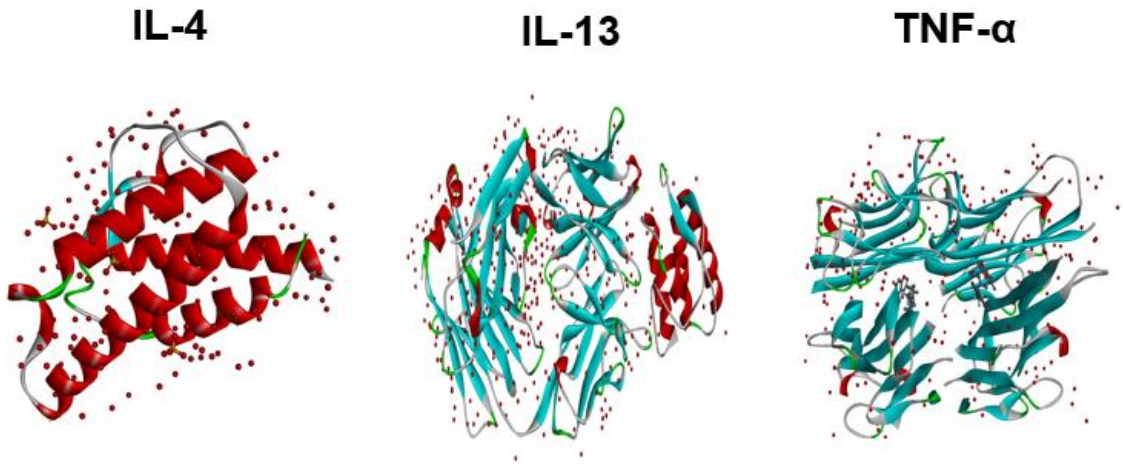

Figure 3. Selected ligands for docking IL-4(4I77), IL-13(2B8U), and TNF-α (2AZ5)

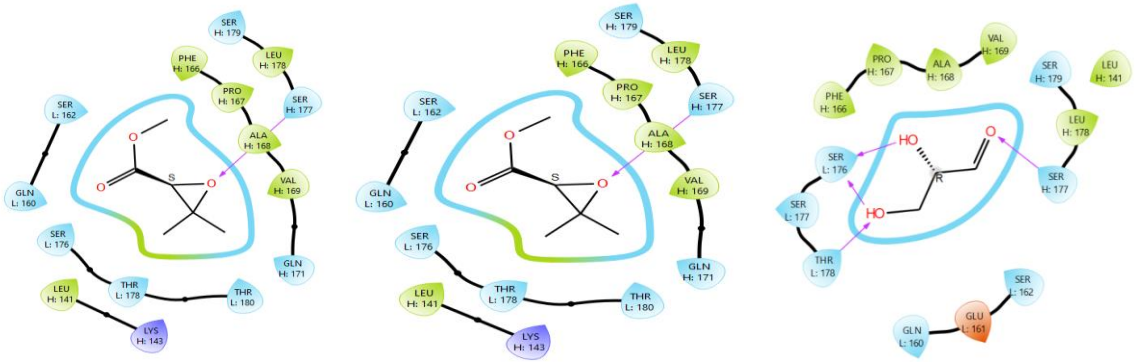

Propanal-2,3-dihydroxy-(*S*) 3,3-Dimethyloxirane-2-carboxylic acid 3-Hexen-2- one 3-methyl

Figure 4. The docking with IL-4 reveals that few compounds have good interactions with target receptors (Table 5).

Table 6. Docking score of top hits with IL-4

Sr./No.	Name	Binding affinity
1	Propanal-2,3-dihydroxy-(*S*)	-5.347
2	3,3-Dimethyloxirane-2-carboxylic acid	-3.237
3	3-Hexen-2- one 3-methyl	-3.553
	Dexamethasone	-3.900

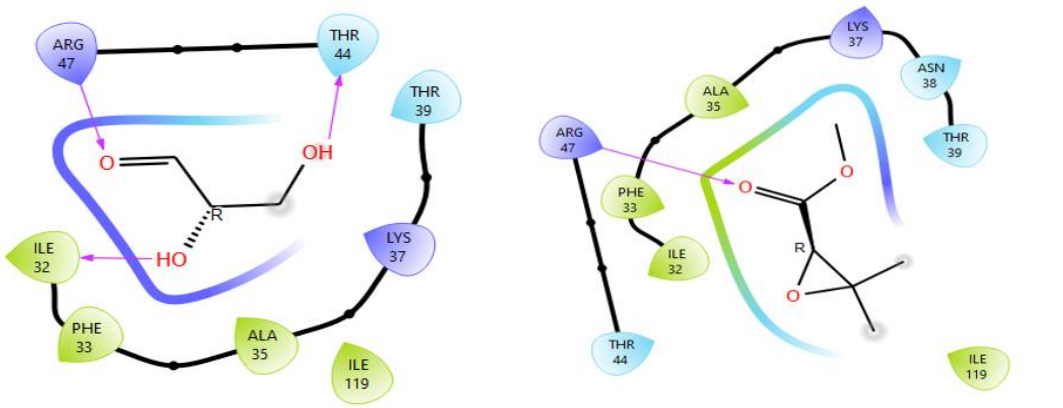

Propanal -2,3-dihydroxy-(S) 3,3-Dimethyloxirane-2-carboxylic acid

Figure 5. The docking with IL-13 reveals that few compounds have good interactions with target receptors (Table 6).

Table 7. Docking score of top hits with IL-13

Sr./No.	Name	Binding affinity
1	Propanal -2,3-dihydroxy-(S)	-3.590
2	3,3-Dimethyloxirane-2-carboxylic acid	-2.631
	Dexamethasone	-3.346

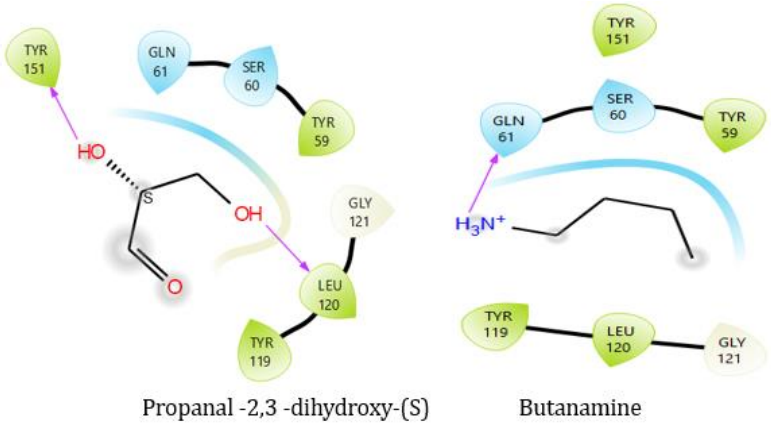

Figure 6. The docking with TNF-α reveals that few compounds have good interactions with target receptors (Table 7).

Table 8. Docking score of top hits TNF-α

Sr./No.	Name	Binding affinity
1	Propanal-2,3-dihydroxy-(*S*)	-3.780
2	Butanamine	-2.629
	Dexamethasone	-5.912

In vitro studies

Antioxidant activity evaluation using DPPH and ABTS assays

The antioxidant potential of the hydroalcoholic extract was assessed through ABTS free radical scavenging assays and DPPH, using ascorbic acid as the standard reference. In the DPPH assay, HAE showed a concentration-dependent increase in radical scavenging activity, ranging from 48.3% to 87.6% inhibition across concentrations of 10 to 100 µg/mL. The standard ascorbic acid demonstrated higher activity, ranging from 91.9% to 99.1% inhibition over the same concentration range. The calculated IC_{50} value of HAE was approximately 10.42 µg/mL, indicating a moderate antioxidant capacity. The assay is based on the reduction of the DPPH radical, evident from the decrease in absorbance at 515 nm, where HAE was effective in quenching free radicals in a dose-responsive manner, as demonstrated in Figure 7. In the ABTS assay, a similar trend was observed where HAE exhibited increasing antioxidant activity with rising concentrations, showing 52% to 94% inhibition from 10 to 100 µg/mL. Ascorbic acid again performed superiorly with inhibition nearing 99% at higher doses. The IC_{50} for HAE in ABTS assay was determined to be approximately 18.04 µg/mL, which, although higher than that in DPPH, still indicates significant antioxidant potential. The ABTS radical cation decolorization assay measures electron-donating ability of antioxidants, and the results affirm that the extract efficiently neutralizes ABTS + radicals, with absorbance read at 750 nm. Together, both assays confirm that the HAE possesses substantial free radical scavenging activity, due to its phenolic constituents, as evidenced by the phytochemical screening. The results support the use of HAE as a natural antioxidant source, and further justify its role in preventing oxidative stress-related cellular damage Figure 8.

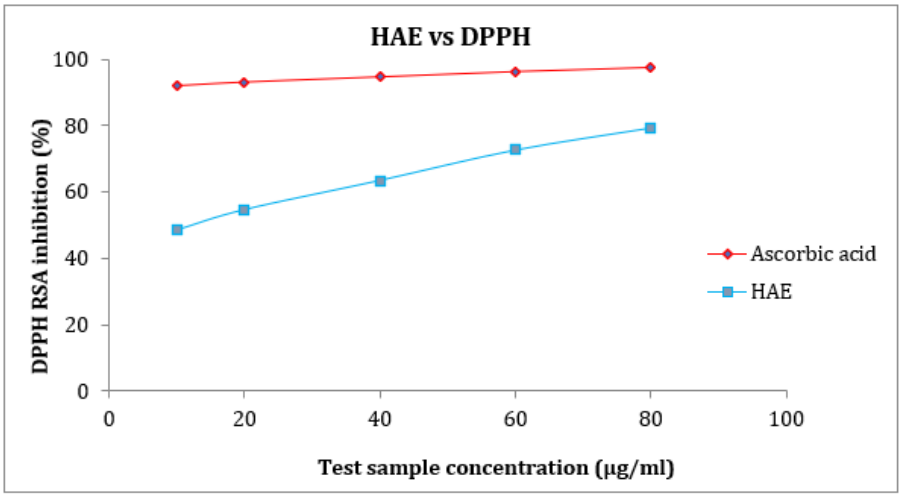

Figure 7. The percentage inhibition of test compounds (HAE) and standard by DPPH radical scavenging activity

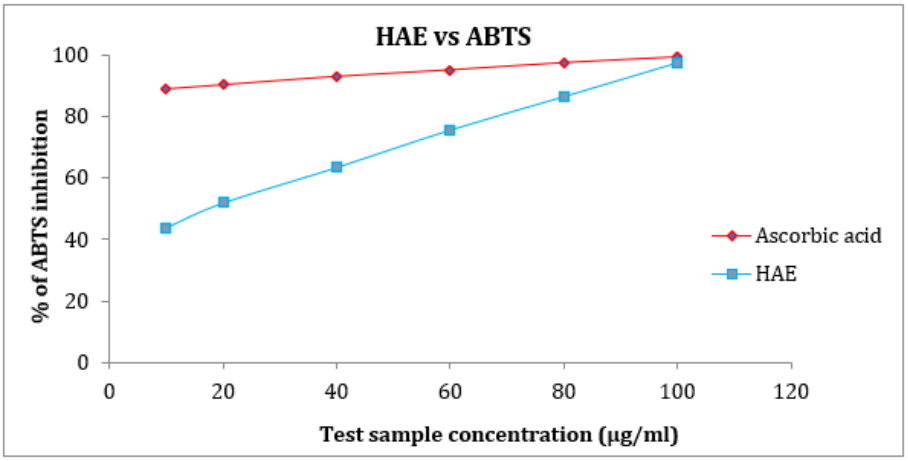

Figure 8. The percentage inhibition of test compounds (HAE) and standard by ABTS radical scavenging activity

Cytotoxicity and nitric oxide inhibition activity

The cytotoxicity assessment of the test compound (HAE) against RAW 264.7 macrophage cells demonstrated excellent biocompatibility across all tested concentrations. MTT assay results revealed that HAE maintained cell viability above 95% at all concentrations (200, 400, 600, 800, and 1,000 µg/mL) after 24 h of treatment, indicating non-cytotoxic nature of the compound Figure 9. The dose-response curve exhibited a linear relationship ($y = 4.444\ln(x) + 122.46$, $R^2 = 0.9903$) with minimal variation in cell viability compared to untreated controls, confirming the safety profile of HAE for subsequent biological evaluations. In contrast, the positive control paclitaxel (163.39 µM) significantly decreased cell viability to about 45% ($p < 0.001$), validating the assay's sensitivity. The nitric oxide inhibition assay demonstrated HAE's potent anti-inflammatory activity, with the compound effectively suppressing LPS-induced NO generation in RAW 264.7 cells in a dose-

dependent manner. Untreated cells produced minimal NO levels (approximately 25 µM), while LPS stimulation dramatically increased NO production to 300 µM ($p < 0.001$). HAE treatment at concentrations of 20, 40, 60, 80, and 100 µg/mL progressively reduced NO production to 200, 175, 125, 100, and 75 µM respectively ($p < 0.05$ for all concentrations), representing 33.3%, 41.7%, 58.3%, 66.7%, and 75% inhibition compared to LPS-treated controls. The standard curve for NO estimation showed excellent linearity ($y = 0.0065x - 0.107$, $R^2 = 0.9982$), ensuring accurate quantification of nitric oxide levels. The combination of non-cytotoxic properties and significant anti-inflammatory activity positions HAE acts as a promising therapeutic candidate for inflammatory disorders, as demonstrated in Figure 10.

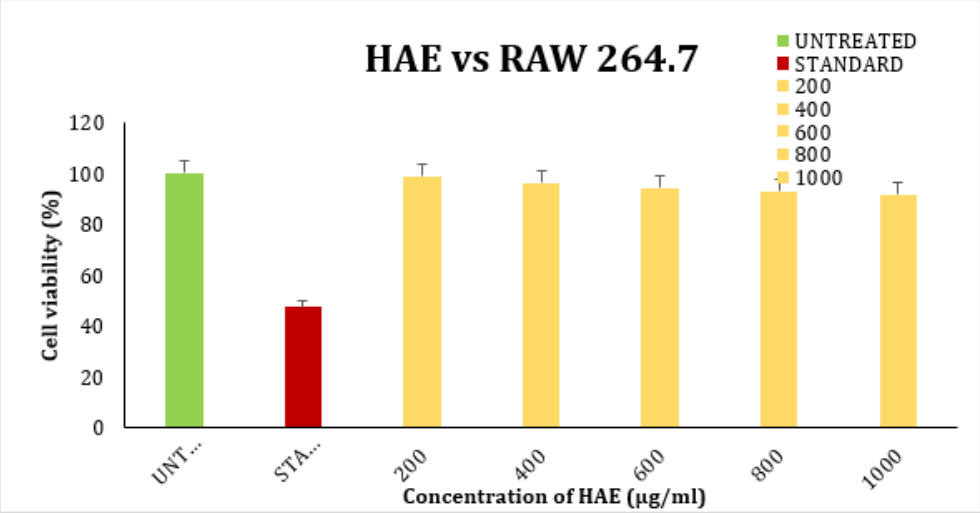

Figure 9. Mean % cell viability of RAW 264.7 cell line after exposing to test compound for 24 h. The dose-response curve exhibited a linear relationship ($y = 4.444\ln(x) + 122.46$, $R^2 = 0.9903$) ($p < 0.001$).

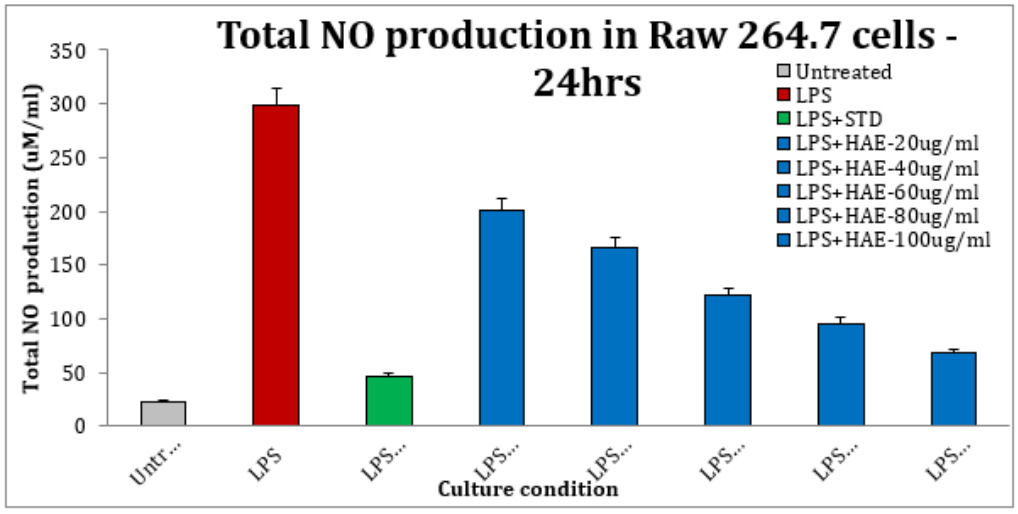

Figure 10. Comparative bar graph representing the total NO reduction in Untreated, LPS treated, LPS+ Dexamethasone and LPS + test treated Raw 264.7 cells after 24 h incubation. The standard curve for NO estimation showed excellent linearity ($y = 0.0065x - 0.107$, $R^2 = 0.9982$) ($p < 0.05$ for all concentrations).

H_2O_2-induced lipid peroxidation in RAW 264.7 cells

The antioxidant potential of HAE was evaluated through its ability to inhibit H_2O_2-induced lipid peroxidation in RAW 264.7 cells, with malondialdehyde (MDA) serving as a biomarker for oxidative stress. H_2O_2 treatment (1 mM) significantly elevated MDA levels to approximately 58 µM compared to untreated controls (12 µM) ($p < 0.001$), indicating substantial oxidative damage. HAE demonstrated potent dose-dependent antioxidant activity, with concentrations of 20, 40, 60, 80, and 100 µg/mL reducing MDA levels to 46, 44, 42, 37, and 27 µM respectively ($p < 0.05$ for all concentrations), representing 20.7%, 24.1%, 27.6%, 36.2%, and 53.4% protection against lipid peroxidation compared to H_2O_2-treated controls (Figure 11).

LPS-induced anti-inflammatory effects

The anti-inflammatory efficacy of HAE was assessed by analyzing key cytokine expression profiles using flow cytometry. LPS stimulation (1 µg/mL) dramatically upregulated pro-inflammatory cytokines, with IL-4 expression increasing to 52% of positive cells compared to 2% in untreated controls ($p < 0.001$), as indicated in Figure 12. HAE treatment (800 µg/mL) significantly suppressed LPS-induced IL-4 expression to 18% ($p < 0.01$), showing 65.4% inhibition compared to LPS-treated controls, while the standard dexamethasone (5 µg/mL) achieved 13% expression, as shown in Figure 13.

Similarly, IL-13 expression was elevated to 95% following LPS stimulation versus 2% in controls ($p < 0.001$) (Figure 14), and HAE treatment reduced this to 75% ($p < 0.05$), representing 21.5% inhibition, whereas dexamethasone achieved 90% expression (Figure 15). Notably, TNF-α expression showed the most pronounced response, with LPS increasing expression to 72% compared to 1% in untreated cells ($p < 0.001$) (Figure 16). HAE treatment reduced TNF-α expression to 38% ($p < 0.01$), demonstrating 47.2% inhibition, while dexamethasone achieved 24% expression (Figure 17).

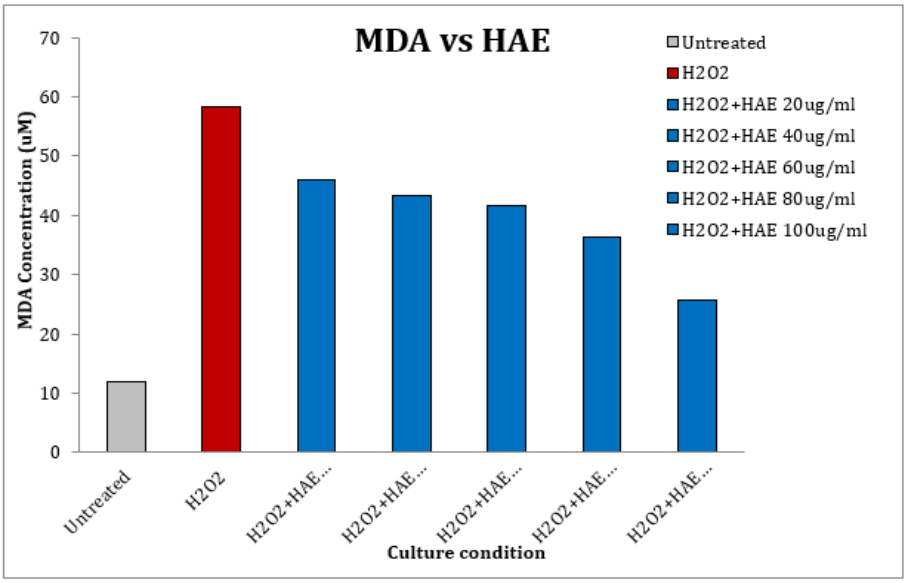

Figure 11. Chart representing the MDA levels in Untreated, H_2O_2 treated, and H_2O_2 + HAE treated Raw 264.7 cells. HAE showed potent dose-dependent antioxidant activity ($p < 0.05$ for all concentrations).

Flow cytometric overlay analysis confirmed the dose-dependent modulation of cytokine expression, with distinct population shifts observed in HAE-treated samples compared to LPS-stimulated controls. These findings collectively demonstrate HAE's dual therapeutic potential as both an antioxidant and anti-inflammatory agent, effectively mitigating oxidative stress-induced cellular damage while modulating key inflammatory mediators in activated macrophages.

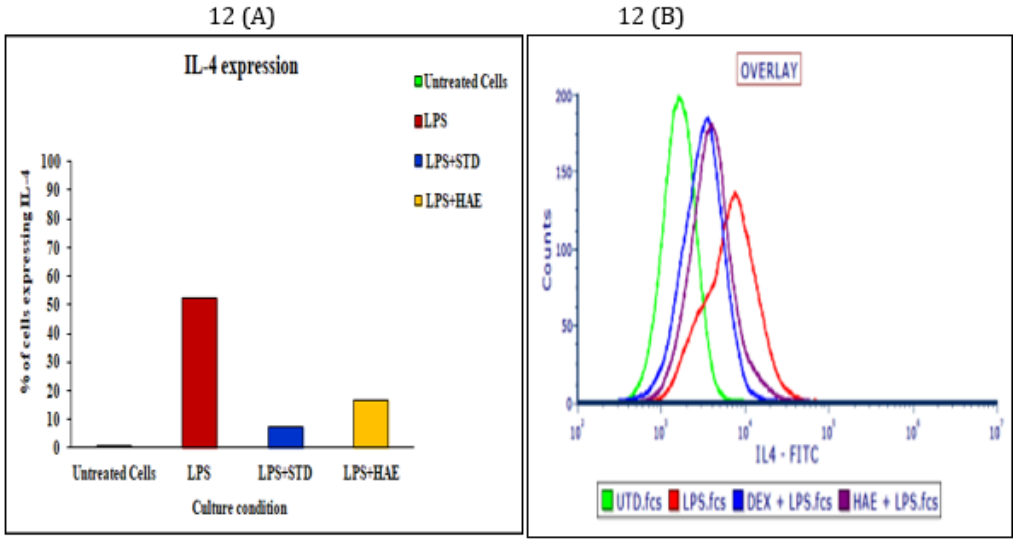

Figure 12. (A) The percent of cells that expressed IL-4 after being stimulated with LPS, treated with the appropriate quantity of standard and sample (HAE). Untreated cells used as negative control. (B) Overlay of intensities of RAW 264.7 cells treated with desired concentration of standard and sample (HAE). Untreated cells used as negative control.

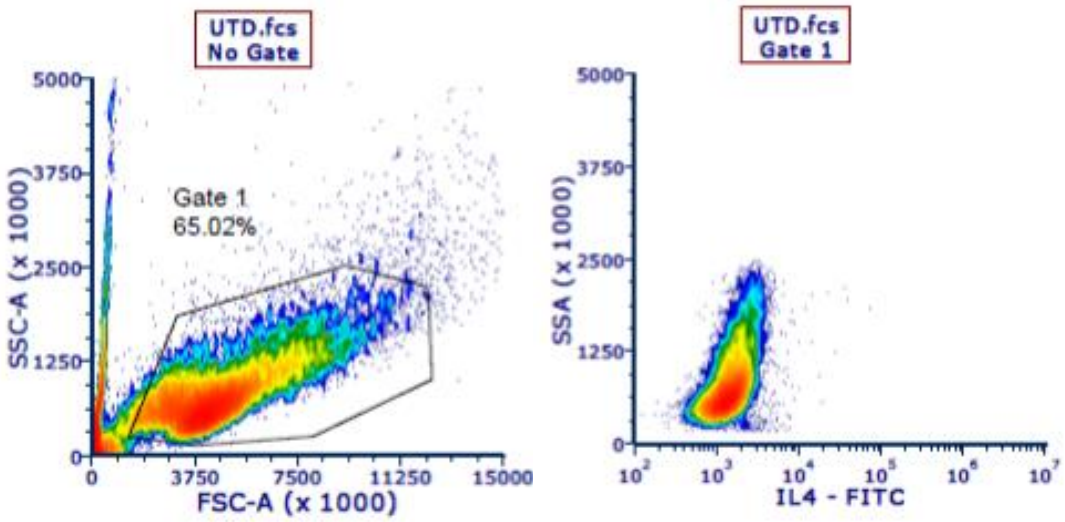

Figure 13. Gating strategy for the analysis of IL-4 expressions on LPS induced RAW 264.7 cell lines by FACS method

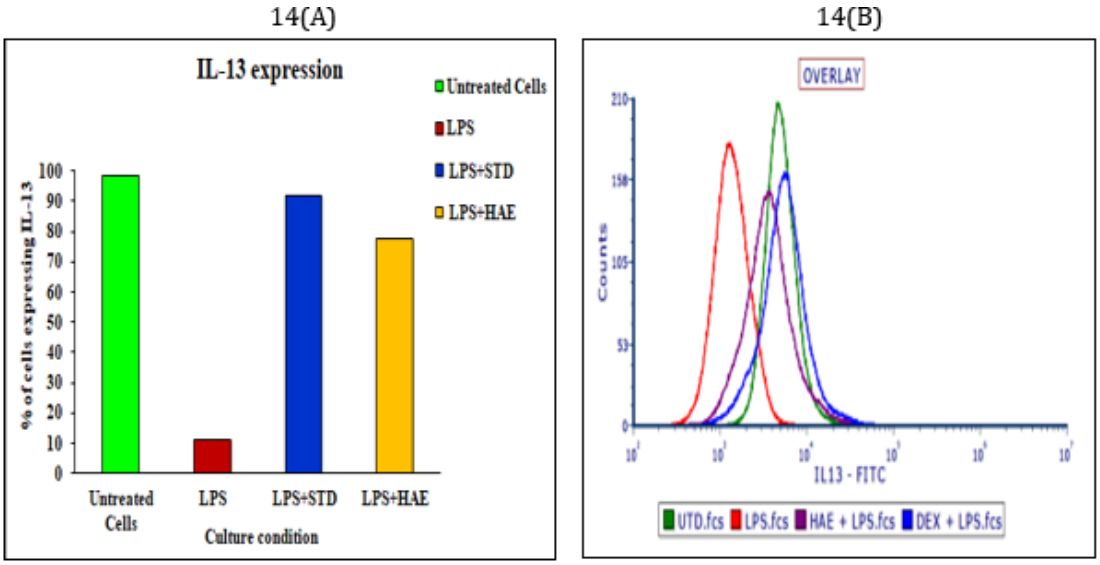

Figure 14. (A) The percent of cells that expressed IL-3 after being stimulated with LPS, treated with the appropriate quantity of standard and sample (HAE). Untreated cells used as negative control. (B) Overlay of intensities of RAW 264.7 cells treated with desired concentration of standard and sample (HAE). Untreated cells used as negative control.

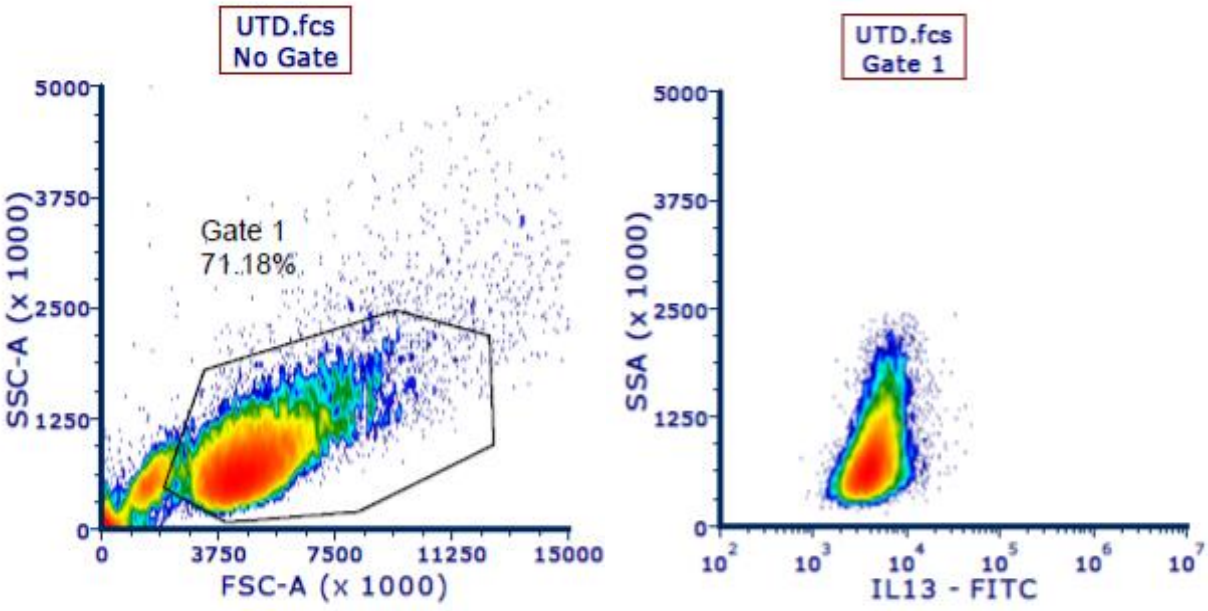

Figure 15. Gating strategy for the analysis of IL-13 expressions on LPS induced RAW 264.7 cell lines by FACS method

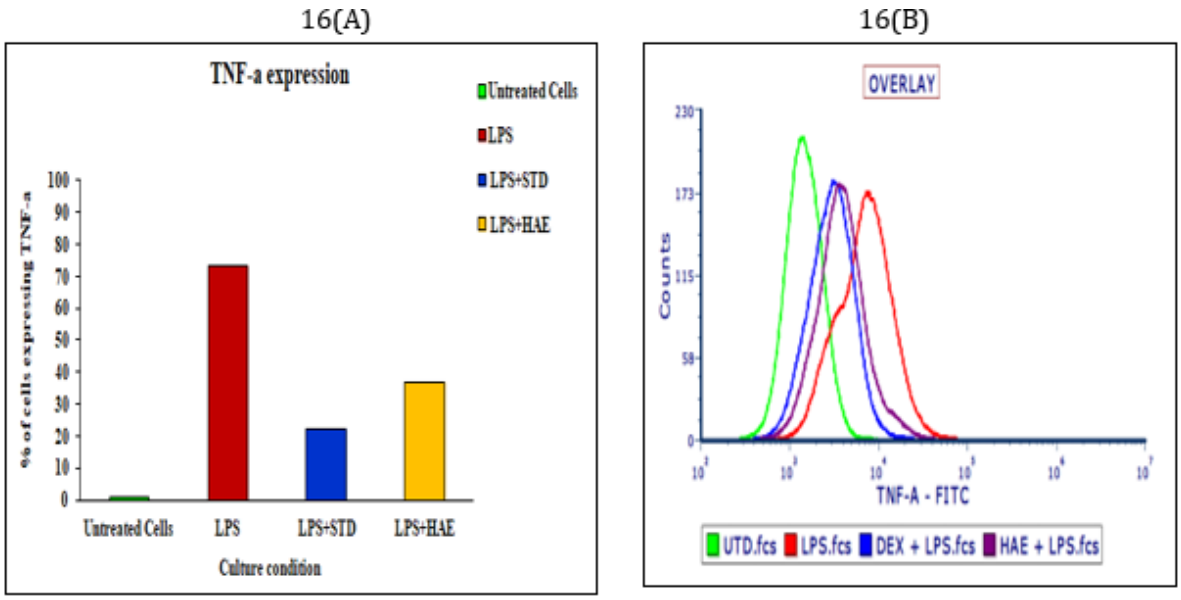

Figure 16. (A) The percent of cells that expressed TNF-α after being stimulated with LPS and treated with the appropriate quantity of standard and sample (HAE). Untreated cells used as negative control, (B) Overlay of intensities of RAW 264.7 cells treated with desired concentration of standard and sample. Untreated cells used as negative control.

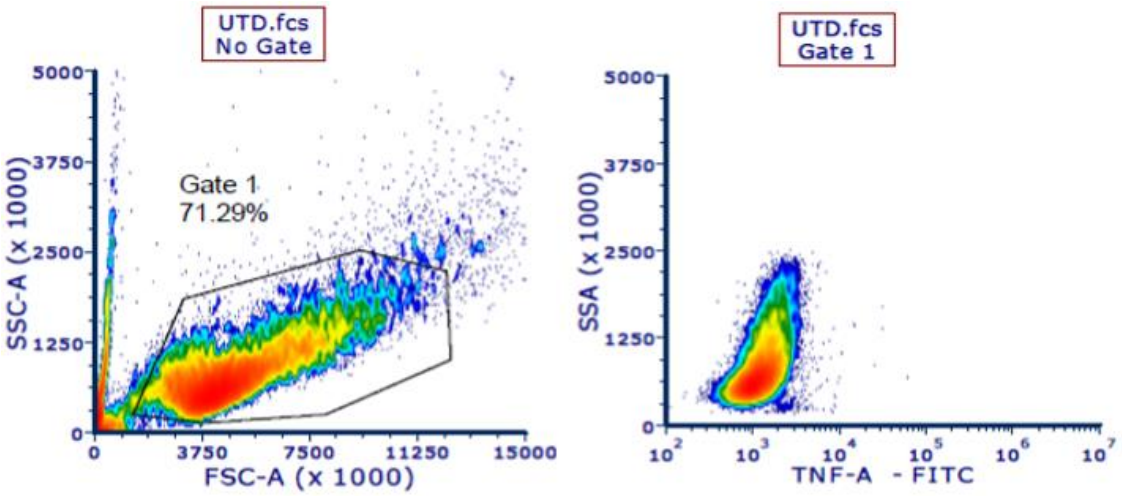

Figure 17. Gating strategy for the analysis of TNF-alpha expressions on LPS induced RAW 264.7 cell lines by FACS method

Discussion

It is well known that LPS-stimulated inflammation causes macrophages to become inflamed. In the present study, the anti-inflammatory effect of the extract which consists of a multiple constituents, was examined through GC-MS, and the confirmation of the binding of the ligands to the target proteins IL-4, IL-13, and TNF-α was performed. Moreover, an *in vitro* investigation employing the LPS stimulated RAW264.7 murine macrophage cell line revealed that the extract markedly and dose-dependently inhibited the increased levels of IL-

4, IL-13, and TNF-α. Macrophages are the main targets of lipopolysaccharide activity and important participants in inflammation. LPS-treated RAW 264.7 murine macrophages are well recognized as an excellent model for studying inflammatory responses. When LPS activates RAW 264.7 murine macrophages, nitric oxide, MDA, and cytokines—inflammatory mediators that control inflammation—increase. Cytokines are inflammatory mediators that regulate inflammation. In this study, it was found that the extract exhibited good inhibitory activity on the LPS-induced generation of NO and MDA in RAW 264.7 cell lines [54,55]. When treating chronic inflammatory conditions, therapeutic blockade of TNF-α is very helpful. Because it increases TNF-α activity and causes nitric oxide, which damages tissue at the site of inflammation, interferon (IFN)-γ, another pleiotropic cytokine, is regarded as a pro-inflammatory cytokine. Furthermore, TNF-α and IL-1 worked together to release inflammatory mediators that target the endothelium [56]. Th2 cell differentiation is promoted by IL-4 and IL-13, which help to regulate the immune system. Thus, as demonstrated by its protective effect in murine models, IL-4 can function as an anti-inflammatory cytokine. Therefore, it is possible to treat autoimmune diseases by targeting IL-4 and IL-13, but they may also be used to treat allergic diseases like asthma [57]. In this study, LPS-activated RAW 264.7 murine macrophages showed lower levels of cytokine expression than normal control. The primary cause of airway inflammation is the overproduction of Th2 cells, which release IL-4, IL-5, and IL-13, subsequently raising IgE production and eosinophilic inflammation. Murine models of airway hyperresponsiveness provide direct evidence of the importance of Th2 cell activation in the pathophysiology of asthma. Asthma's allergen-specific immune response is characterized by the immediate production of IL-4 by T cells and the activation of B cells, which raises IgE secretion. Since IL-13 causes airway hyperresponsiveness (AHR) and various structural changes in chronic asthma, it is currently a key therapeutic target for the treatment of allergic asthma [58,59]. The study proves that the presence of various bioactive compounds in the hydroalcoholic extract attributed to the potent antioxidant and antiasthmatic properties of the seeds of *Emblica officinalis*. The future prospect of the study is to investigate the properties using OVA induced models for the seed extract which can lead to isolation of active constituents responsible for the anti-asthmatic activity [60]. These findings demonstrated that the gooseberry seed extract effectively inhibited IL-4 and IL-13 activity, cytokines that are key mediators in IgE synthesis, eosinophil activation, mucus hypersecretion, and airway remodeling. This mechanism of action shows a close parallel with the effects observed in biological therapies targeting these interleukins, such as lebrikizumab and dupilumab, which have been shown to reduce airway inflammation and asthma severity by modulating the IL-4/IL-13 signaling pathway. The comparable inhibitory response observed in this study suggests that phytoconstituents from gooseberry seeds may exert similar immunomodulatory potential through interference with these shared receptor pathways, offering a promising natural alternative for managing Th2-driven airway inflammation [61].

Conclusion

Based on the phytochemical analysis and characterization, the phytoconstituents of hydroalcoholic extract of *Emblica officinalis* seeds have led compounds that bind to the target proteins that is identified by molecular docking. The *in vitro* assays performed prove that the hydroalcoholic extract possesses antioxidant activity. The cytotoxicity of the test compound,

(HAE) was evaluated by the MTT assay. The experimental results suggested that the test compound (HAE) was non-toxic against the RAW 264.7 cells after 24 h of incubation. The anti-inflammatory effect of test compound (HAE) was analyzed by assessing IL-4, IL-13, TNF-alpha expression in LPS induced RAW 264.7 cell lines using FACS method. The results of this study indicated that test sample (HAE) exerted for anti- inflammatory effects in LPS-stimulated RAW 264.7 cell line.

Acknowledgements

The authors would like to sincerely thank Karpagam Academy of Higher Education, Coimbatore and JSS Academy of Higher Education and Research, Mysuru for the facilities provided in conducting this research.

Funding

This work is not financially supported.

Conflict of Interest

The authors declared no conflicts of interest in this work.

ORCID

Elango Kannan
https://orcid.org/0000-0001-6330-8342
Mumtha Logesh
https://orcid.org/0009-0004-9626-6803

References

[1] Olsthoorn, S.E., van Krimpen, A., Hendriks, R.W., Stadhouders, R. Chronic inflammation in asthma: Looking beyond the th2 cell. *Immunological Reviews*, **2025**, 330(1), e70010.
[2] Croisant, S. Epidemiology of asthma: Prevalence and burden of disease. *Heterogeneity in Asthma*, **2013**, 17-29.
[3] Pastore, D., Lupia, C., D'Amato, M., Bruni, A., Garofalo, E., Longhini, F., Gallelli, L., Vatrella, A., Pelaia, G., Pelaia, C. Emerging biological treatments for asthma. *Expert Opinion on Emerging Drugs*, **2025**, 30(2), 87-97.
[4] Sihombing, J.L., Gea, S., Wirjosentono, B., Agusnar, H., Pulungan, A.N., Herlinawati, H., Yusuf, M., Hutapea, Y.A. Characteristic and catalytic performance of Co and Co-Mo metal impregnated in Sarulla natural zeolite catalyst for hydrocracking of MEFA rubber seed oil into biogasoline fraction. Catalysts, 2020, 10, 121**.**
[5] GBD 2015 Disease and Injury Incidence and Prevalence Collaborators. Global, regional, and national incidence, prevalence, and years lived with disability for 310 diseases and injuries, 1990–2015: a systematic analysis for the Global Burden of Disease Study 2015. *The Lancet*, **2016**, 388(10053), 1545–1602.
[6] Jin H J. Biological treatments for severe Asthma. *Yeungnam University Journal of Medicine,* **2020**, 37(4), 262–268.
[7] Diamant, Z., Jesenak, M., Hanania, N.A., Heaney, L.G., Djukanovic, R., Ryan, D., Quirce, S., Backer, V., Gaga, M., Pavord, I., Antolín-Amérigo, D. EUFOREA pocket guide on the diagnosis and management of asthma: an educational and practical tool for general practitioners, non-respiratory physicians, paramedics and patients. *Respiratory Medicine*, **2023**, 218, 107361.
[8] Schramm, B., Ehlken, B., Smala, A., Quednau, K., Berger, K., Nowak, D. Cost of illness of atopic asthma and seasonal allergic rhinitis in germany: 1-yr retrospective study. *European Respiratory Journal*, **2003**, 21(1), 116-122.
[9] Spergel, J.M., Paller, A.S. Atopic dermatitis and the atopic march. *Journal of Allergy and Clinical Immunology*, **2003**, 112(6), S118-S127.
[10] O'connell, E. The burden of atopy and asthma in children. *Allergy*, **2004**, 59, 7-11.
[11] Ismaila, A.S., Sayani, A.P., Marin, M., Su, Z. Clinical, economic, and humanistic burden of asthma in canada: A systematic review. *BMC Pulmonary Medicine*, **2013**, 13(1), 70.
[12] Berger, P. Physiopathologie de l'asthme sévère: Quelles cibles moléculaires pour les biothérapies? *Bulletin de l'Académie Nationale de Médecine*, **2023**, 207(5), 605-611.
[13] Yang, Y., Jia, M., Ou, Y., Adcock, I.M., Yao, X. Mechanisms and biomarkers of airway epithelial cell damage in asthma: A review. *The Clinical Respiratory Journal*, **2021**, 15(10), 1027-1045.
[14] Global Initiative for Asthma (GINA). Global Strategy for Asthma Management and Prevention (Workshop Report), **2006**.

[15] Anderson, G.P. Endotyping asthma: New insights into key pathogenic mechanisms in a complex, heterogeneous disease. *The Lancet*, **2008**, 372(9643), 1107-1119.
[16] Hambly, N., Nair, P. Monoclonal antibodies for the treatment of refractory asthma. *Current Opinion in Pulmonary Medicine*, **2014**, 20(1), 87-94.
[17] Pelaia, C., Heffler, E., Crimi, C., Maglio, A., Vatrella, A., Pelaia, G., Canonica, G.W. Interleukins 4 and 13 in asthma: Key pathophysiologic cytokines and druggable molecular targets. *Frontiers in Pharmacology*, **2022**, 13, 851940.
[18] Shankar, A., McAlees, J.W., Lewkowich, I.P. Modulation of il-4/il-13 cytokine signaling in the context of allergic disease. *Journal of Allergy and Clinical Immunology*, **2022**, 150(2), 266-276.
[19] Moran, A., Pavord, I.D. Anti-il-4/il-13 for the treatment of asthma: The story so far. *Expert Opinion on Biological Therapy*, **2020**, 20(3), 283-294.
[20] Habib, N., Pasha, M.A., Tang, D.D. Current understanding of asthma pathogenesis and biomarkers. *Cells*, **2022**, 11(17), 2764.
[21] Vimala, Y., Rachel, K.V., Pramodini, Y., Umasankar, A. Usage of indian gooseberry (*Emblica officinalis*) seeds in health and disease. *Nuts and Seeds in Health and Disease Prevention*, **2011**, 663-670.
[22] Govind, P., Pandey, S. Phytochemical and toxicity study of *Emblica officinalis* (amla). *International Research Journal of Pharmacy*, **2011**, 2(3), 270-272.
[23] Dogra, K.S., Chauhan, S., Jalal, J.S. Assessment of indian medicinal plants for the treatment of asthma. *Journal of Medicinal Plants Research*, **2015**, 9(32), 851-862.
[24] Dasaroju, S., Gottumukkala, K.M. Current trends in the research of *Emblica officinalis* (amla): A pharmacological perspective. *Internationa Journal of Pharmaceutical Sciences Review and Research*, **2014**, 24(2), 150-159.
[25] Khandelwal, K.R. Practical pharmacognosy. *Book*, **2008**.
[26] Faruq, M.O., Rahim, A., Arifuzzaman, M., Ghosh, G.P. Phytochemicals screening, nutritional assessment and antioxidant activities of a. Viridis l. And a. Spinosus l. Leaves: A comparative study. *Journal of Agriculture and Food Research*, **2024**, 18, 101341.
[27] Gupta, S., Basavan, D., Nataraj, S.K.M., Raju, K.R.S., Babu, U., LM, S.K., Gupta, R. Assessment of inhibitory potential of pothos scandens l. On ovalbumin-induced airway hyperresponsiveness in BALB/C mice. *International Immunopharmacology*, **2014**, 18(1), 151-162.
[28] Trease, G., Evans, W. Pharmacognosy. Brailliar tiridel and macmillian publishers. London, uk. **1989**.
[29] Balamurugan, V., Fatima, S., Velurajan, S. A guide to phytochemical analysis. *International Journal of Advance Research and Innovative Ideas in Education*, **2019**, 5(1), 236-245.
[30] Arawande, J.O., Akinnusotu, A., Alademeyin, J.O. Extractive value and phytochemical screening of ginger (zingiber officinale) and turmeric (curcuma longa) using different solvents. *International Journal of Tradational and Natural Medicines*, **2018**, 8(1), 13-22.
[31] Abbas, A., Naqvi, S.A.R., Rasool, M.H., Noureen, A., Mubarik, M.S., Tareen, R.B. Phytochemical analysis, antioxidant and antimicrobial screening of seriphidium oliverianum plant extracts. *Dose-response*, **2021**, 19(1), 15593258211004739.
[32] Khalid, M., Amayreh, M., Sanduka, S., Salah, Z., Al-Rimawi, F., Al-Mazaideh, G.M., Alanezi, A.A., Wedian, F., Alasmari, F., Shalayel, M.H.F. Assessment of antioxidant, antimicrobial, and anticancer activities of sisymbrium officinale plant extract. *Heliyon*, **2022**, 8(9).
[33] Shalini, K., Ilango, K. Preliminary phytochemical studies, GC-MS analysis and in vitro antioxidant activity of selected medicinal plants and its polyherbal formulation. *Pharmacognosy Journal*, **2021**, 13(3).
[34] Priyadharshini, S., Swaroop, A.K., Jubie, S., Jawahar, N., Divecha, V. Molecular docking and cytotoxicity interactions of naringenin and its nano-structured lipid carriers in erα positive breast cancer. *Indian Journal of Biochemistry and Biophysics (IJBB)*, **2023**, 60(2), 141-147.
[35] Yamauchi, M., Kitamura, Y., Nagano, H., Kawatsu, J., Gotoh, H. DPPH measurements and structure—activity relationship studies on the antioxidant capacity of phenols. *Antioxidants*, **2024**, 13(3), 309.
[36] Schlesier, K., Harwat, M., Böhm, V., Bitsch, R. Assessment of antioxidant activity by using different in vitro methods. *Free Radical Research*, **2002**, 36(2), 177-187.
[37] Silva, F., Veiga, F., Cardoso, C., Dias, F., Cerqueira, F., Medeiros, R., Paiva-Santos, A.C. A rapid and simplified dpph assay for analysis of antioxidant interactions in binary combinations. *Microchemical Journal*, **2024**, 202, 110801.
[38] Lang, Y., Gao, N., Zang, Z., Meng, X., Lin, Y., Yang, S., Yang, Y., Jin, Z., Li, B. Classification and antioxidant assays of polyphenols: A review. *Journal of Future Foods*, **2024**, 4(3), 193-204.
[39] Yan, H., Hou, W., Lei, B., Liu, J., Song, R., Hao, W., Ning, Y., Zheng, M., Guo, H., Pan, C. Ultrarobust stable abts radical cation prepared using spore@ cu-tma biocomposites for antioxidant capacity assay. *Talanta*, **2024**, 276, 126282.

[40] Sriklung, K., Apiratikul, N., Samosorn, S., Narkwichean, A., Watanapokasin, R. Lupalbigenin inhibiting nf-κb translocation associated with anti-inflammatory responses in lipopolysaccharide stimulated raw 264.7 macrophages. *Journal of the Medical Association of Thailand*, **2022**, 105.
[41] Ilaghi, M., Sharifi, I., Sharififar, F., Sharifi, F., Oliaee, R.T., Babaei, Z., Meimamandi, M.S., Keyhani, A., Bamorovat, M. The potential role and apoptotic profile of three medicinal plant extracts on leishmania tropica by mtt assay, macrophage model and flow cytometry analysis. *Parasite Epidemiology and Control*, **2021**, 12, e00201.
[42] Moon, H.R., Chung, M.J., Park, J.W., Cho, S.M., Choi, D.J., Kim, S.M., Chun, M.H., Kim, I.B., Kim, S.O., Jang, S.J., Park, Y.I. Antiasthma effects through anti-inflammatory action of acorn (Quercus acutissima Carr.) *in vitro* and *in vivo*. *Journal of Food Biochemistry*, **2013**, 37(1), 108–118.
[43] Joo, T., Sowndhararajan, K., Hong, S., Lee, J., Park, S.Y., Kim, S., Jhoo, J.W. Inhibition of nitric oxide production in lps-stimulated raw 264.7 cells by stem bark of ulmus pumila l. *Saudi Journal of Biological Sciences*, **2014**, 21(5), 427-435.
[44] Achoui, M., Appleton, D., Abdulla, M.A., Awang, K., Mohd, M.A., Mustafa, M.R. In vitro and in vivo anti-inflammatory activity of 17-o-acetylacuminolide through the inhibition of cytokines, nf-κb translocation and ikkβ activity. *PloS one*, **2010**, 5(12), e15105.
[45] Taira, J., Nanbu, H., Ueda, K. Nitric oxide-scavenging compounds in agrimonia pilosa ledeb on lps-induced raw264. 7 macrophages. *Food Chemistry*, **2009**, 115(4), 1221-1227.
[46] Tian, Y., Zhou, S., Takeda, R., Okazaki, K., Sekita, M., Sakamoto, K. Anti-inflammatory activities of amber extract in lipopolysaccharide-induced raw 264.7 macrophages. *Biomedicine & Pharmacotherapy*, **2021**, 141, 111854.
[47] Mas-Bargues, C., Escriva, C., Dromant, M., Borras, C., Vina, J. Lipid peroxidation as measured by chromatographic determination of malondialdehyde. Human plasma reference values in health and disease. *Archives of Biochemistry and Biophysics*, **2021**, 709, 108941.
[48] Ghonimi, N.A., Elsharkawi, K.A., Khyal, D.S., Abdelghani, A.A. Serum malondialdehyde as a lipid peroxidation marker in multiple sclerosis patients and its relation to disease characteristics. *Multiple Sclerosis and Related Disorders*, **2021**, 51, 102941.
[49] Ahmad, G., Hassan, R., Dhiman, N., Ali, A. Assessment of anti-inflammatory activity of 3-acetylmyricadiol in lpsstimulated raw 264.7 macrophages. *Combinatorial Chemistry & High Throughput Screening*, **2022**, 25(1), 204-210.
[50] Sornsenee, P., Chatatikun, M., Mitsuwan, W., Kongpol, K., Kooltheat, N., Sohbenalee, S., Pruksaphanrat, S., Mudpan, A., Romyasamit, C. Lyophilized cell-free supernatants of lactobacillus isolates exhibited antibiofilm, antioxidant, and reduces nitric oxide activity in lipopolysaccharide-stimulated raw 264.7 cells. *PeerJ*, **2021**, 9, e12586.
[51] Yoon, S.B., Lee, Y.J., Park, S.K., Kim, H.C., Bae, H., Kim, H.M., Ko, S.G., Choi, H.Y., Oh, M.S., Park, W. Anti-inflammatory effects of Scutellaria baicalensis water extract on LPS-activated RAW 264.7 macrophages. *Journal of Ethnopharmacology*, **2009**, 125(2), 286–290.
[52] Kwon, O.K., Lee, M.Y., Yuk, J.E., Oh, S.R., Chin, Y.W., Lee, H.K., Ahn, K.S. Anti-inflammatory effects of methanol extracts of the root of Lilium lancifolium on LPS-stimulated RAW264.7 cells. *Journal of Ethnopharmacology*, **2010**, 130(1), 28–34.
[53] Uprety, L.P., Park, Y.H., Jang, Y.J. Autoantigen spermatid nuclear transition protein 1 enhances pro-inflammatory cytokine production stimulated by anti-DNA autoantibodies in macrophages. *European Journal of Inflammation*, **2022**, 20, 1-9.
[54] Monga, S., Fares, B., Yashaev, R., Melamed, D., Kahana, M., Fares, F., Weizman, A., Gavish, M. The effect of natural-based formulation (NBF) on the response of raw264. 7 macrophages to LPS as an in vitro model of inflammation. *Journal of Fungi*, **2022**, 8(3), 321.
[55] Khirallah, S.M., Ramadan, H.M., Shawky, A., Qahl, S.H., Baty, R.S., Alqadri, N., Alsuhaibani, A.M., Jaremko, M., Emwas, A.-H., Saied, E.M. Development of novel 1, 3-disubstituted-2-thiohydantoin analogues with potent anti-inflammatory activity; in vitro and *in silico* assessments. *Molecules*, **2022**, 27(19), 6271.
[56] Zhao, G., Zhang, T., Ma, X., Jiang, K., Wu, H., Qiu, C., Guo, M., Deng, G. Oridonin attenuates the release of pro-inflammatory cytokines in lipopolysaccharide-induced raw264. 7 cells and acute lung injury. *Oncotarget*, **2017**, 8(40), 68153.
[57] Hu, X.D., Yang, Y., Zhong, X.G., Zhang, X.H., Zhang, Y.N., Zheng, Z.P., Zhou, Y., Tang, W., Yang, Y.F., Hu, L.H. Anti-inflammatory effects of z23 on lps-induced inflammatory responses in raw264. 7 macrophages. *Journal of Ethnopharmacology*, **2008**, 120(3), 447-451.
[58] Jeon, C.M., Shin, I.S., Shin, N.R., Hong, J.M., Kwon, O.K., Kim, H.S., Oh, S.R., Myung, P.K., Ahn, K.S. Siegesbeckia glabrescens attenuates allergic airway inflammation in lps-stimulated raw 264.7 cells and ova induced asthma murine model. *International immunopharmacology*, **2014**, 22(2), 414-419.
[59] Lee, J.W., Seo, K.H., Ryu, H.W., Yuk, H.J., Park, H.A., Lim, Y., Ahn, K.S., Oh, S.R. Anti-inflammatory effect of stem bark of paulownia tomentosa steud. In

lipopolysaccharide (lps)-stimulated raw264. 7 macrophages and lps-induced murine model of acute lung injury. *Journal of Ethnopharmacology*, **2018**, 210, 23-30.
[60] Amaral-Machado, L., Oliveira, W.N., Moreira-Oliveira, S.S., Pereira, D.T., Alencar, E.N., Tsapis, N., Egito, E.S.T. Use of natural products in asthma treatment. *Evidence-Based Complementary and Alternative Medicine*, **2020**, 2020(1), 1021258.
[61] Bagnasco, D., Ferrando, M., Varricchi, G., Passalacqua, G., Canonica, G.W. A critical evaluation of anti-il-13 and anti-il-4 strategies in severe asthma. *International Archives of Allergy and Immunology*, **2016**, 170(2), 122-131.

HOW TO CITE THIS MANUSCRIPT
E. Kannan, M. Logesh, P. S. Evaluation of Anti-Asthmatic Potential of *Emblica Officinalis* Seed Extract in RAW 264.7 Cell Lines. *Asian Journal of Green Chemistry*, 10 (4) 2026, 565-588.
DOI: https://doi.org/10.48309/ajgc.2026.553890.1848
URL: https://www.ajgreenchem.com/article_238876.html